Disorder-enhanced exciton delocalization in an extended dendrimer

V. Pouthier

Disorder-enhanced exciton delocalization in an extended dendrimer

Vincent Pouthier*
Institut UTINAM, Université de Franche-Comté, CNRS UMR 6213, 25030 Besançon Cedex, France
(Received 17 March 2014; published 28 August 2014)

The exciton dynamics in a disordered extended dendrimer is investigated numerically. Because a homogeneous dendrimer exhibits few highly degenerate energy levels, a dynamical localization arises when the exciton is initially located on the periphery. However, it is shown that the disorder lifts the degeneracy and favors a delocalization-relocalization transition. Weak disorder enhances the delocalized nature of the exciton and improves any quantum communication, whereas strong disorder prevents the exciton from propagating in accordance with the well-known Anderson theory.

DOI: 10.1103/PhysRevE.90.022818 PACS number(s): 89.75.Fb, 03.67.Hk, 71.35.−y, 71.23.An

I. INTRODUCTION

A dendrimer is an engineered polymer whose hyperbranched structure on a nanoscale looks like the fractal patterns that occur in the plant kingdom [1–4]. It consists of several dendritic branches, called dendrons, that emanate out from a central core. Each dendron is formed by long molecular chains organized in a self-similar fashion. It exhibits branching points where the chain splits into two or three chains, increasing the generation number, and its periphery is occupied by functional terminal groups. Consequently, the dendrimer involves a series of chemical shells whose flexibility, porosity, and surface functionalization can be used to perform many applications [4].

In that context, it has been suggested that exciton-mediated energy transport could be exploited to design artificial light-harvesting complexes [5–23]. The main idea consists in the functionalization of the terminal groups by chromophores that favor light harvesting. As in natural photosynthetic antenna, the absorbed light yields Frenkel excitons that propagate along the dendrons. The excitons converge toward the central core, where chemical fuel is finally produced [24,25].

However, besides practical interests, a dendrimer constitutes a physical realization of a complex network. Studying the exciton dynamics is thus of fundamental importance because of its formal resemblance with a continuous time quantum walk (CTQW) [26]. During the past few years, CTQW in complex networks has become a very popular research topic owing to its potential use in the development of algorithms in quantum information processing [27–31]. Therefore, to judge the efficiency of a CTQW, the fundamental question is whether the exciton propagates coherently or localizes along the network. Although this problem still remains open, recent research suggests that the localized or delocalized nature of the exciton depends on general features such as the network topology, the initial implementation of the CTQW, and the presence of disorder [26].

In an extended dendrimer, when the initial wave function is either uniformly distributed over the periphery or localized on the central core, quantum interferences arise because multiple scatterings occur each time the exciton tunnels from one generation to another. As a result, the exciton localizes when the generation number exceeds a critical value, indicating that only small-size dendrimers allow efficient communication between the core and the surface [32]. By contrast, in a compact dendrimer, the exciton delocalizes coherently between the periphery and the core, its dynamics being mapped onto that of a linear chain [33]. Its behavior results from the interplay between the dispersion and the occurrence of quantum recurrences, making possible quantum communication. However, when the exciton is initially located on a single surface site, its propagation is stopped and it remains confined over the few sites that surround the excited site [33]. As shown by Mulken *et al.* [34], this specific localization takes place in finite networks with a few highly degenerate eigenenergies that yield specific quantum interferences. Not restricted to dendrimers, this effect was observed in star graphs [35] and Apollonian networks [36].

As in solid-state physics, localization may also arise when the network is perturbed by random defects. But the influence of the disorder is quite subtle. Indeed, at first sight, in accordance with the well-known concept of localization transition due to Anderson [37,38], the disorder acts as a negative ingredient. For instance, disordered site energies completely stop the CTQW in linear chains [39], discrete rings [40], and binary trees [41]. Similarly, the disorder prevents efficient communication between the roots of two glued trees [42,43]. In other cases, the disorder behaves as a positive ingredient that enhances the delocalized nature of the exciton. For instance, in tree graphs similar to dendrimers, a weak disorder yields extended states through fluctuation-enabled resonances between states that initially may appear to be localized [44,45]. In a Watts-Strogatz network with small-world behavior [46], the efficiency of a CTQW is enhanced when the rewiring probability turns on [47]. Finally, when bonds are randomly added to a star graph, the CTQW spreads more [48].

In the present paper, a simple model is thus introduced for describing the interplay between the initial localization of a CTQW and the presence of disorder inherent to any realistic network. To proceed, we investigate the exciton dynamics in a small-size extended dendrimer. Although the exciton localizes when it is initially created on a surface site of a homogeneous dendrimer, it is shown that the disorder favors a delocalization-relocalization transition. A weak disorder enhances the delocalized nature of the exciton and improves the quantum communication, whereas a strong disorder prevents the exciton from propagating and stops any CTQW.

*vincent.pouthier@univ-fcomte.fr

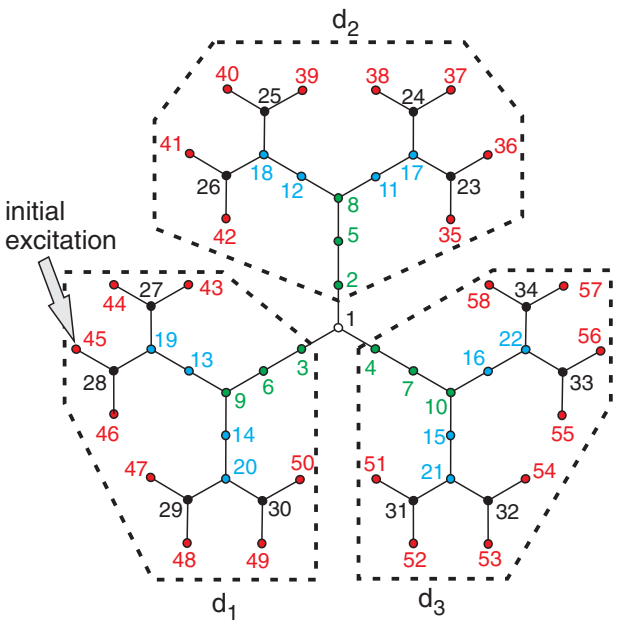

FIG. 1. (Color online) Polyphenylacetylene extended dendrimer D58. Each circle defines a phenyl ring, whereas a connecting line stands for an acetylene group involving two single bonds and one triple bond.

The paper is organized as follows. In Sec. II, the disordered dendrimer is introduced and the exciton Hamiltonian is defined. Then, the relevant observables required for characterizing the dynamics are described. The problem is solved numerically in Sec. III, where a detailed analysis of the influence of the disorder is performed. The numerical results are finally discussed in Sec. IV.

II. THEORETICAL BACKGROUND

A. Exciton Hamiltonian

The simple network we consider is the extended polyphenylacetylene dendrimer $D58$, displayed in Fig. 1. It is built from linearly connected diphenylacetylene units and involves $N = 58$ phenyl rings. The connectivity of the branching points is equal to three so that $D58$ has a threefold symmetry around its central core. It consists of three dendrons, d_1, d_2, and d_3, and it is formed by four generations. The first generation involves nine phenyl rings organized into three shells that encircle the central core. The second generation consists of 12 rings distributed into two shells. The third and the fourth generations involve a single shell built with 12 and 24 rings, respectively.

The phenyl rings define sites for a network model that describes the dynamics of Frenkel excitons [5–12]. Each site $x = 1, \ldots, N$ is occupied by a two-level system that accounts for the electronic properties of a phenyl ring. Let $|x\rangle$ denote the first excited state of the xth two-level system and $\hbar\omega_x$ the corresponding energy. Within the local basis $\{|x\rangle\}$, the exciton dynamics is governed by a tight-binding Hamiltonian written as [5–12] (in unit $\hbar = 1$)

$$H = \sum_x \left(\omega_x |x\rangle\langle x| + \sum_{x'} \Phi_{xx'} [|x\rangle\langle x'| + |x'\rangle\langle x|] \right), \quad (1)$$

where $\Phi_{xx'}$ is the exciton hopping matrix. It reduces to a constant Φ when x and x' correspond to nearest neighbor phenyl rings connected by a diphenylacetylene leg; otherwise it vanishes.

According to the standard Anderson model [37,38], the disorder is introduced by assuming that the site energies $\{\omega_x\}$ are independent random variables uniformly distributed on the interval $[\omega_0 - W/2, \omega_0 + W/2]$. The symbol $\langle \cdots \rangle$, denoting an ensemble average over the disorder, ω_0 is the mean value $\langle \omega_x \rangle$ of each site energy. Similarly, W measures the strength of the disorder and it defines the corresponding variance $\langle (\omega_x - \omega_0)^2 \rangle = W^2/12$.

B. Quantum dynamics

In this work, we consider the particular situation in which the exciton is initially localized on the surface site $x_0 = 45$ (see Fig. 1). Note that the case of an initial wave function uniformly distributed over all the surface site has been investigated recently [32]. The exciton dynamics is described by the evolution operator $U(t)$, whose behavior is governed by the Schrödinger equation, as

$$i\dot{U}_{xx_0}(t) = \omega_x U_{xx_0}(t) + \sum_{x'} \Phi_{xx'} U_{x'x_0}(t). \quad (2)$$

The matrix element $U_{xx_0}(t)$ defines the exciton wave function on site x at time t provided that the exciton was located on site x_0 at $t = 0$. Equation (2) can be solved easily by diagonalizing the system Hamiltonian, Eq. (1), for each disordered configuration. For a specific configuration, let $|\chi_k\rangle$ denote the kth eigenstate of H and ω_k the corresponding eigenvalue, with $k = 1, \ldots, N$. The evolution operator is expressed in terms of the stationary wave functions $\chi_{kx} = \langle x|\chi_k\rangle$ as

$$U_{xx_0}(t) = \sum_{k=1}^{N} \chi_{kx} \chi^*_{kx_0} e^{-i\omega_k t}. \quad (3)$$

From the knowledge of both the evolution operator and the eigenstates, different observables can be computed. First, we focus our attention on the exciton density $P_{x|x_0}(t) = |U_{xx_0}(t)|^2$. It represents the probability of observing the exciton on site x at time t and provides key information on the way the energy flows along the network. Then, in finite-size networks, $P_{x|x_0}(t)$ does not converge to a stationary value because a unitary dynamics arises [49]. Instead, it fluctuates around a long time average distribution called the limiting probability $\bar{P}_{x|x_0}$. It is defined as

$$\bar{P}_{x|x_0} = \sum_{k=1}^{N} \sum_{k'=1}^{N} \chi_{kx} \chi^*_{k'x} \chi_{k'x_0} \chi^*_{kx_0} \delta_{\omega_k,\omega_{k'}}, \quad (4)$$

where $\delta_{\omega_k,\omega_{k'}} = 1$ if $\omega_k = \omega_{k'}$ and zero otherwise. The limiting probability gives a good estimate of the time-dependent probability and is a key quantity to prove the localized nature of the exciton [33]. Finally, we study the time-dependent participation ratio $R(t) = 1/\sum_{x=1}^{N} |U_{xx_0}(t)|^4$ that represents the number of sites visited by the exciton during the quantum walk [47,50]. Equal to unity when the wave function is localized on a single site, it reaches N when the exciton becomes uniformly distributed over the dendrimer.

The exciton density, the limiting probability, and the time-dependent participation ratio are the central objects of the present study. They give information about the way the excitonic wave function propagates along the network after its initial implementation. Their knowledge allows us to characterize the influence of the disorder and thus to know whether the exciton localizes or delocalizes, as illustrated in the next section.

III. NUMERICAL RESULTS

In Figs. 2–4, we first present numerical results obtained for three specific energy landscapes drawn by randomly distributed site energies for $W = 0.0$ (ordered dendrimer), $W = 0.5$ (weakly disordered dendrimer), and $W = 5.0$ (strongly disordered dendrimer), respectively.

Figure 2 shows the time evolution of the probability $P_d(t)$ to observe the exciton on the dendron $d = d_1$, d_2, and d_3. When $W = 0.0$ [Fig. 2(a)], the exciton remains localized on the excited dendron. The probability $P_{d_1}(t)$ exhibits small-amplitude high-frequency fluctuations around a limiting value

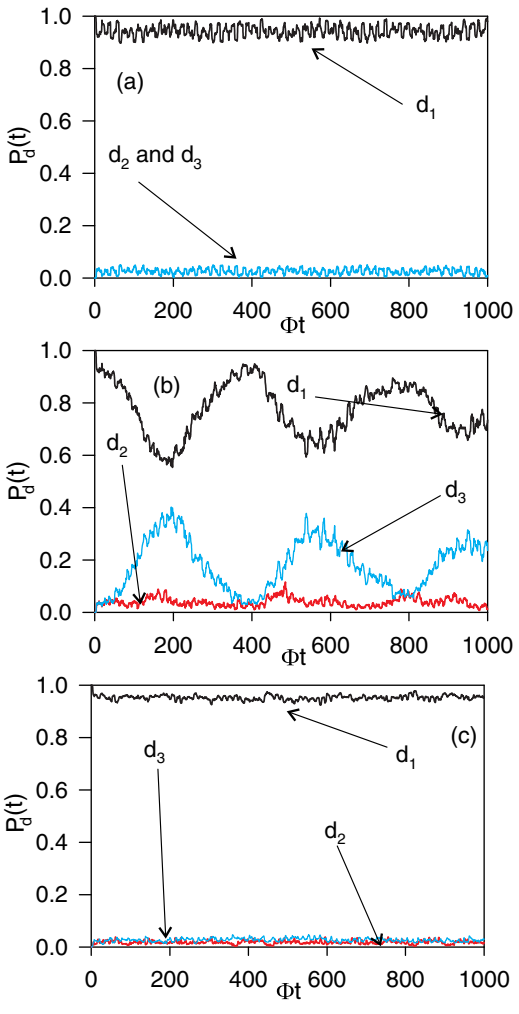

FIG. 2. (Color online) Time evolution of the probability $P_d(t)$ to observe the exciton on the dendron $d = d_1$ (black curve), $d = d_2$ (red [dark gray] curve), and $d = d_3$ (blue [light gray] curve) for different disorder strengths: (a) $W = 0.0$, (b) $W = 0.5\Phi$, and (c) $W = 5.0\Phi$.

$\bar{P}_{d_1} = 0.9428$. The probabilities to observe the exciton on d_2 and d_3 are identical due to the threefold symmetry. They slightly oscillate around a negligible limiting value equal to 0.02561. In other words, after the initial excitation of the periphery of d_1, 94.28% of the exciton population stays confined on d_1 and only 5.22% of the population reaches the two other dendrons, reflecting an inefficient quantum communication. Note that the population of the central core remains very small during the simulation (not drawn), its limiting value being approximately equal to 0.48%. This result contrasts with previous calculations, which revealed that 84% of the exciton population can reach the central core when the initial wave function is uniformly distributed over the periphery of the dendrimer [32].

In a weakly disordered dendrimer ($W = 0.5\Phi$), a different behavior occurs, as displayed in Fig. 2(b) for a particular configuration of the disorder. Indeed, $P_{d_1}(t)$ shows small-amplitude oscillations around a slowly varying function. This function scales as a periodic function whose period is approximately equal to $400\Phi^{-1}$. Consequently, after half a period, $P_{d_1}(t)$ deviates significantly from unity. It decreases to 0.5539 for $t = 197.80\Phi^{-1}$, indicating that about half of the density left the excited dendron. In fact, this particular configuration yields a coherent transfer between d_1 and d_3. The probability $P_{d_3}(t)$ behaves as a sine function whose maximum value, which occurs at $t = 197.80\Phi^{-1}$, is equal to 0.3997. In that case, the population of d_2 remains negligible, its maximum value being equal to 0.0370. Note that such a behavior survives in the intermediate disorder regime. For instance, for the same disordered configuration but with $W = 2.0\Phi$, a coherent exciton transfer still arises between d_1 and d_3, although the role played by d_2 is no longer negligible (not drawn). However, in a strongly disordered dendrimer ($W = 5.0\Phi$), the localized nature of the exciton recurs [Fig. 2(c)]. The probability $P_{d_1}(t)$ shows small-amplitude fluctuations around a limiting value close to unity. Approximately 95.31% of the exciton population remains confined on the excited dendron whereas the population of d_2 and d_3 reaches 1.81% and 2.70%, respectively.

The behavior of the time-dependent participation ratio $R(t)$ is illustrated in Fig. 3. When $W = 0.0$, as time elapses, $R(t)$ first increases from unity. It reaches 6.10 for $t = 3.0\Phi^{-1}$ [Fig. 3(a)]. Then, it exhibits high-frequency small-amplitude oscillations around a limiting value equal to 4.15, indicating that the exciton localizes over few sites that surround the excited site. Note that the maximum value of $R(t)$ is equal to 6.57 and it occurs at $t = 89.6\Phi^{-1}$. As shown in Fig. 3(b) for $W = 0.5\Phi$, a different behavior occurs for a weakly disordered configuration. Indeed, $R(t)$ shows high-frequency small-amplitude oscillations around a slowly varying sinelike function. The participation ratio is now able to take larger values. It reaches 23.00 for $t = 226.0\Phi^{-1}$, indicating that the exciton can visit almost half of the sites of the dendrimer. Note that we have verified that such a behavior remains for a disorder strength ranging between 0.5Φ and 2.5Φ. For instance, for $W = 2.0\Phi$, $R(t)$ reaches 25.12 for $t = 652.8\Phi^{-1}$ (not drawn). Finally, in the strong disorder limit ($W = 5.0\Phi$), $R(t)$ behaves as in a homogeneous dendrimer. It fluctuates around a limiting value equal to 4.29 and it reaches a maximum value equal to 8.12 for $t = 420.2\Phi^{-1}$.

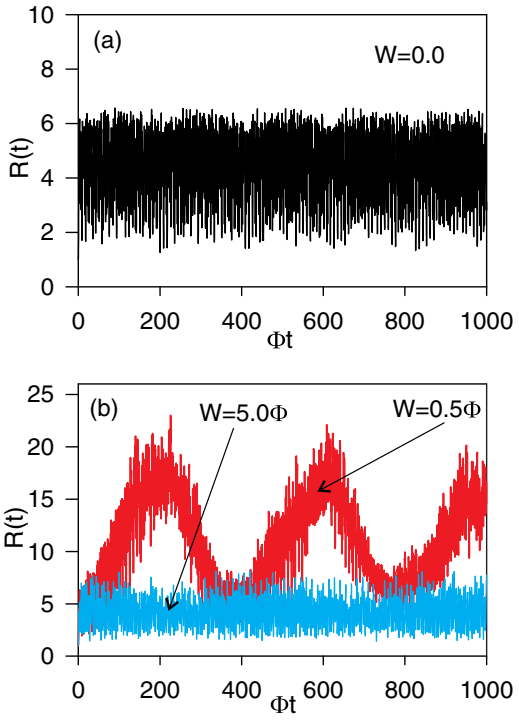

FIG. 3. (Color online) Time evolution of the time dependent participation ratio $R(t)$ for (a) $W = 0.0$ and for (b) $W = 0.5\Phi$ (red curve) and $W = 5.0\Phi$ (blue curve).

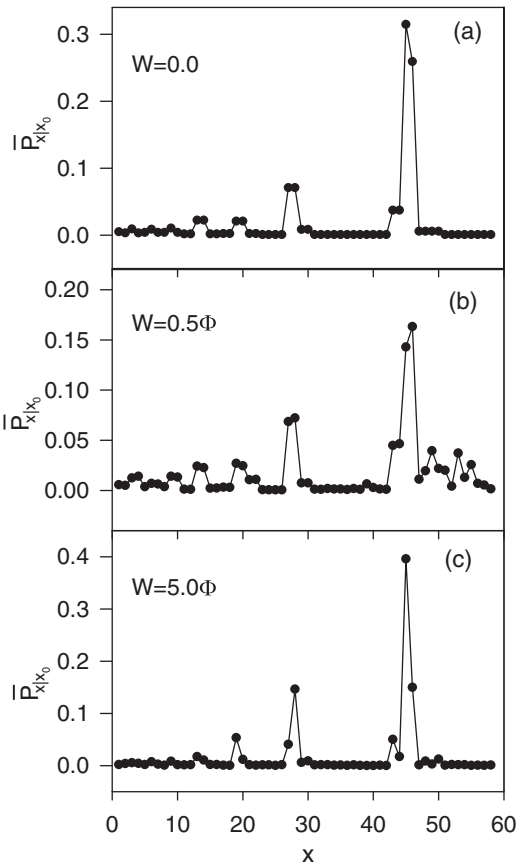

FIG. 4. Limiting probability $\bar{P}_{x|x_0}$ for (a) $W = 0.0$, (b) $W = 0.5\Phi$, and (c) $W = 5.0\Phi$.

The limiting probability is displayed in Fig. 4 for different W values. When $W = 0.0$ [Fig. 4(a)], the distribution exhibits peaks that reveal that the exciton is mainly localized over a few sites that surround the excited site. The distribution is rather large on the sites 45 and 46. Then, it is relatively important on sites 27, 28, 43, 44 and, to a lesser extent, 19 and 13. These eight sites define the so-called excited region where the probability of observing the exciton is equal to 83.24%.

In the weak disorder regime ($W = 0.5\Phi$), for a particular configuration of the disorder, the probability to observe the exciton in the excited region represents no more than 58.88%. In that case, the limiting distribution broadens and additional peaks occur [Fig. 4(b)]. These peaks account for two different features. First, the exciton is now able to explore a larger region inside the excited dendron. In particular, it can reach the surface sites 47, 48, 49, and 50, the limiting probability of occupying these sites being equal to 9.20%. Then, and this is what is noteworthy, the probability to observe the exciton on the other dendrons is no longer negligible. For instance, the probability that the exciton occupies the periphery of d_3 is equal to 11.36%. Similarly, specific peak reveals that the exciton can reach the branching points 10, 21, and 22 with higher probability. Finally, in the strong disorder regime ($W = 5.0\Phi$), the localized nature of the limiting distribution recurs [Fig. 4(c)]. As in a homogeneous dendrimer, the probability of observing the exciton in the excited region reaches 87%. Note that the exciton mainly localizes on three sites, namely sites 45, 46, and 28.

The previous results were obtained for a particular energy landscape drawn by specific randomly distributed site energies. By carrying out various simulations, we clearly observed that most weakly disordered configurations enhance the exciton delocalization, whereas most strongly disordered landscapes favor relocalization. Nevertheless, for a fixed W value, different configurations may give rise to different dynamical behaviors. Therefore, to determine the general effect produced by the random defects, an ensemble average over the disorder is now realized.

Figure 5 shows the W dependence of the average limiting probability $\langle \bar{P}_{d_1} \rangle$ that the exciton occupies the excited dendron. As observed previously, $\langle \bar{P}_{d_1} \rangle = 94.28\%$ when $W = 0.0$, indicating that the exciton remains confined on d_1 and localizes on the excited region. However, when the disorder switches on, different regimes take place. For a very weak disorder, a delocalization process suddenly arises, giving rise to a discontinuity in the curve $\langle \bar{P}_{d_1} \rangle$ vs W. The probability $\langle \bar{P}_{d_1} \rangle$ decreases from 94.28% for $W = 0.0$ to 82.97% for $W = 0.001\Phi$. In the same time, $\langle \bar{P}_{d_2} \rangle$ and $\langle \bar{P}_{d_3} \rangle$ suddenly increase from 2.61% for $W = 0.0$ to 8.29% for $W = 0.001\Phi$. As W increases again, the exciton delocalization is enhanced so that $\langle \bar{P}_{d_1} \rangle$ slightly decreases, whereas $\langle \bar{P}_{d_2} \rangle$ and $\langle \bar{P}_{d_3} \rangle$ increase. Such a behavior occurs provided that W remains smaller than 1.1Φ. Then, when W ranges between 1.1Φ and 1.6Φ, $\langle \bar{P}_{d_1} \rangle$ becomes almost independent of the strength of the disorder. It reaches a minimum value equal to 76.50%. Similarly, $\langle \bar{P}_{d_2} \rangle$ and $\langle \bar{P}_{d_3} \rangle$ reach a plateau whose value is approximately equal to 11.33%. When W exceeds 1.6Φ, a relocalization process takes place so that $\langle \bar{P}_{d_2} \rangle$ and $\langle \bar{P}_{d_3} \rangle$ decrease to the detriment

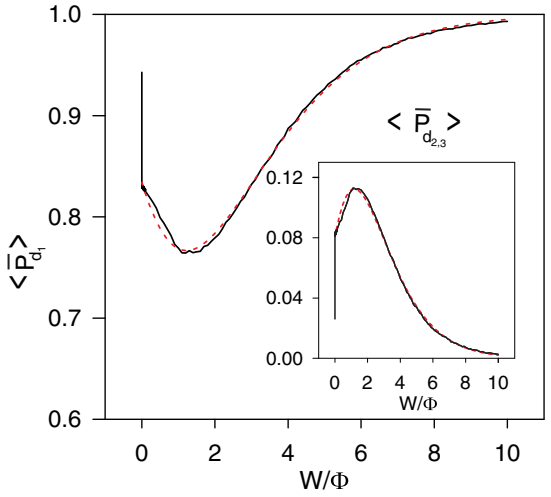

FIG. 5. (Color online) W dependence of the average limiting probability $\langle \bar{P}_{d_1} \rangle$ that the exciton occupies d_1. The average was carried out by considering 10^4 disordered configurations. The inset shows the average limiting probability of observing the exciton on d_2 and d_3. Dashed red (gray) curves correspond to the analytical law discussed in the text [see Eq. (5)].

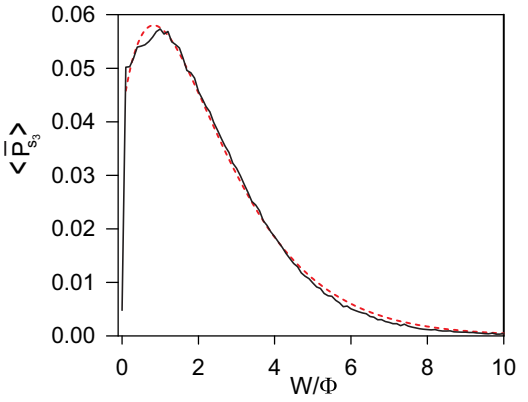

FIG. 6. (Color online) W dependence of the average limiting probability $\langle \bar{P}_{s_3} \rangle$ of observing the exciton on the surface of the dendron d_3. The average was carried out by considering 10^4 disordered configurations. The dashed red (gray) curve corresponds to the analytical law discussed in the text.

of $\langle \bar{P}_{d_1} \rangle$ that increases. For $W \approx 3.0\Phi$, one recovers the average limiting probabilities obtained for $W = 0^+$, that is, for a very weak disorder. Then, when $W \approx 5.5\Phi$, the average limiting probabilities behave as in a homogeneous dendrimer. Finally, for a strong disorder ($W > 5.5\Phi$), the exciton strongly localizes in the close neighborhood of the excited site. For instance, for $W = 10.0\Phi$, $\langle \bar{P}_{d_1} \rangle = 99.31\%$, with 83.56% of the population being localized on three sites: $x = 45$, 46, and 28.

Provided that $W > 0$, the previous behavior is quite well captured by the following law (see dashed curves in Fig. 5):

$$\left\langle \bar{P}_{d_1} \right\rangle \approx 1 - a(W + b)^2 e^{-W/W^*} \tag{5}$$

with $a \approx 0.09$, $b \approx 1.33$, and $W^* \approx 1.27$. Because the limiting probability that the exciton occupies the central core remains very small whatever the value of W (not drawn), one obtains $\langle \bar{P}_{d_2} \rangle = \langle \bar{P}_{d_3} \rangle \approx (1 - \langle \bar{P}_{d_1} \rangle)/2$. Note that we have verified that the limiting population of the central core is a continuous function of W. Equal to 0.48% for $W = 0.0$, it first increases with W and reaches a maximum value equal to 0.97% for $W \approx 1.4\Phi$. Then, when W increases again, it decreases and tends to zero.

To illustrate the way the disorder enhances the propagation of the exciton, Fig. 6 displays the W dependence of the average limiting probability $\langle \bar{P}_{s_3} \rangle$ of observing the exciton on the surface of the dendron d_3. In a homogeneous dendrimer ($W = 0.0$), $\langle \bar{P}_{s_3} \rangle = 0.48\%$, indicating that it is unlikely that the exciton reaches the surface of d_3 from the excited site. By contrast, when W switches on, a discontinuity occurs in the curve so that $\langle \bar{P}_{s_3} \rangle$ suddenly increases to 5.02% for $W = 0.1\Phi$. Then, when W increases again, $\langle \bar{P}_{s_3} \rangle$ increases until it reaches a maximum value equal to 5.73% for $W \approx \Phi$. At this step, one clearly sees the key role played by the disorder. The limiting probability of observing the exciton on the surface of d_3 is multiplied by more than one order of magnitude when compared with what happens in a homogeneous dendrimer. Finally, in the strong disorder limit, $\langle \bar{P}_{s_3} \rangle$ becomes a decreasing function of W. It behaves as in a homogeneous dendrimer when $W \approx 6.6\Phi$ and it finally tends to zero in the very strongly disordered regime. Note that, for $W > 0$, such a behavior is quite well captured by the law $\langle \bar{P}_{s_3} \rangle \approx a(W + b)^2 \exp(-W/W^*)$, with $a \approx 0.03$, $b \approx 1.26$, and $W^* \approx 1.06$ (see dashed curve in Fig. 6).

Finally, Fig. 7 displays the W dependence of $P_{\max}$ that represents the average of the maximum value of the probability $P_{56|45}(t)$ to observe the exciton on site $x = 56$ (see Fig. 1). Note that the simulation was carried out over a time interval fixed to $5 \times 10^3 \Phi^{-1}$. When $W = 0.0$, $P_{\max} = 0.58\%$, indicating that the communication between two ends of a homogeneous dendrimer is very inefficient. However, when W switches on, $P_{\max}$ suddenly increases so that a better exciton propagation takes place. As observed in Figs. 5 and 6,

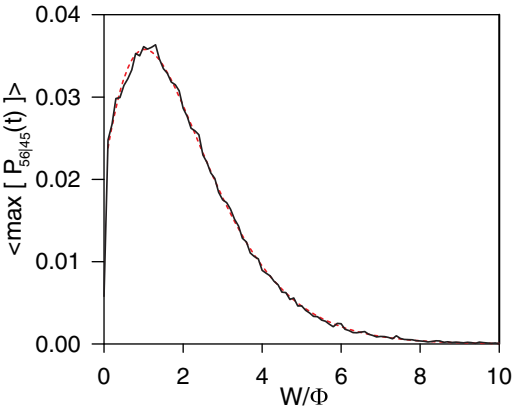

FIG. 7. (Color online) W dependence of the average of the maximum value of the probability $P_{56|45}(t)$ to observe the exciton on site $x = 56$. The simulation was carried out using 5×10^4 time steps over a time interval fixed to $5 \times 10^3 \Phi^{-1}$. The average was realized by considering 5000 disordered configurations. The dashed red curve corresponds to the analytical law discussed in the text.

a discontinuity occurs in the curve $P_{\max}$ vs W. Therefore, when $W = 0.01\Phi$, $P_{\max}$ is multiplied by a factor equal to 4.3 and it reaches 2.48%. Then, when W increases again, $P_{\max}$ increases. When W ranges between Φ and 1.4Φ, $P_{\max}$ reaches a maximum plateau whose value is approximately equal to 3.60%. In the strongly disordered regime, $P_{\max}$ becomes a decaying function of W. When $W \approx 4.7\Phi$, one recovers what happens in a homogeneous dendrimer. Then, in the very strongly disordered regime, $P_{\max}$ converges to zero by exhibiting an exponential tail. Once again, when $W > 0$, this behavior is quite well represented by the law $P_{\max} \approx a(W + b)^2 \exp(-W/W^*)$, with $a \approx 0.03$, $b \approx 0.79$, and $W^* \approx 0.91$ (see dashed curve in Fig. 7).

IV. DISCUSSION AND CONCLUSION

The numerical results clearly show that the exciton dynamics exhibits different facets depending on the strength of the disorder. In a homogeneous dendrimer, a dynamical localization arises when the exciton is initially located on a surface site. Similarly to what happens in a compact dendrimer [33], the exciton localizes over the few sites that define the excited region which surrounds the excited site. Consequently, the efficiency of any quantum communication protocol linking two ends of the dendrimer will be rather poor, with the corresponding CTQW being confined in the neighborhood of its initial implementation. When the dendrimer is perturbed by random site energies, a threshold value $W^* \approx 1.25\Phi$ of the strength of the disorder discriminates between two regimes. Surprisingly, a weak disorder ($W < W^*$) hinders the localization mechanism that naturally occurs in a homogeneous network. It enhances the propagation of the exciton so that the particle becomes able to explore a larger region around the excited site. It thus improves the quantum communication and facilitates the spreading of a CTQW. By contrast, in the strong disorder regime ($W > W^*$), the dynamical localization recurs in accordance with what is expected from the Anderson theory. The exciton becomes trapped over a few sites around the excited site, the size of the excited region decreasing with the strength of the disorder.

To interpret these features, let us mention that the diversity of the dynamics mainly results from the sensitivity of the exciton eigenstates to the energy landscape drawn by the random site energies. Indeed, in accordance with the laws of quantum mechanics, the dynamics is governed by the evolution operator $U_{xx_0}(t)$ that defines the probability amplitude that the exciton tunnels from x_0 to x during time t [see Eq. (3)]. This amplitude is the sum over the elementary probability amplitudes associated with the different paths that the exciton can follow to tunnel. A given path defines a transition through a stationary state $|\chi_k\rangle$. It involves the weight of the localized states $|x\rangle$ and $|x_0\rangle$ in the eigenstate $|\chi_k\rangle$ and depends on the eigenenergy ω_k through a phase factor. Consequently, the way any observable evolves in time will result from the quantum interferences between the paths followed by the exciton. Depending on whether the dendrimer is homogeneous or disordered, different eigenstates will produce specific interference patterns so that various regimes will arise ranging from a localized regime to a delocalized regime.

In a homogeneous dendrimer, the Hamiltonian H exhibits two kinds of eigenstates. First, eight nondegenerate energy levels characterize eigenstates that are totally symmetric with respect to the threefold symmetry around the central core. In such a state, the exciton wave function is uniformly distributed over each shell that forms the dendrimer. As shown previously, these states can be mapped onto those of a linear chain involving eight sites, each site referring to a particular shell of the dendrimer [32]. Then, the remaining 50 eigenstates are grouped into 13 degenerate energy levels. The degeneracy of most of these levels is equal to two or three. Nevertheless, three highly degenerate energy levels stand out, the corresponding energies being equal to ω_0, $\omega_0 + \sqrt{2}\Phi$, and $\omega_0 - \sqrt{2}\Phi$. The degeneracy of the level with energy ω_0 is equal to 14, whereas the degeneracy of the levels with energy $\omega_0 \pm \sqrt{2}\Phi$ reduces to six.

In that context, the behavior of the exciton depends on the way the initial state decomposes on the eigenstates. When the initial wave function is uniformly distributed over a particular shell, only the totally symmetric eigenstates are excited. The dynamics can be mapped onto that of a finite-size chain so that the excitonic wave delocalizes from shell to shell. Its behavior is thus governed by reflection effects, by lattice dispersion, and by the occurrence of quantum recurrences [32]. A different behavior occurs when the exciton is initially localized on a surface site. In that case, although the initial state still decomposes on the eight totally symmetric eigenstates, we have verified that it mainly involves eigenstates that belong to the three highly degenerate energy levels. Such a decomposition selects particular paths that the exciton follows to propagate. Therefore, it turns out that specific quantum interferences between these particular paths give rise to the localization of the exciton, as observed in the previous section. The propagation is stopped and the exciton remains confined over the few sites that surround the excited site. This specific localization is not restricted to extended dendrimers. As shown by Mulken and coworkers [34] using general arguments, it occurs in complex networks whose density of states contains few highly degenerate eigenvalues. The degeneracies of the eigenvalues dominate the temporal behavior so that a quantum walk has a large probability of staying where it was implemented, resulting in a low transport efficiency.

For understanding the influence of the disorder, a systematic analysis of the excitonic eigenstates was performed for different disordered configurations. These studies allowed us to highlight general trends and to propose a simple scenario for explaining our results, especially in the weakly disordered regime. In that regime, the dynamics mainly results from the modification of the highly degenerate eigenstates responsible for the dynamical localization in the homogeneous case. Indeed, weak disorder only slightly modifies the nondegenerate totally symmetric states whose extended nature remains owing to the finite size of the dendrimer. By contrast, it strongly affects the degenerate states whose modification cannot be taken into account using perturbation theory, even if the disorder is extremely weak. In that context, it turns out that the weak disorder breaks the threefold symmetry around the central core. It raises the degeneracy of the three highly degenerate energy levels, resulting in the occurrence

of states *a priori* localized on various parts of the dendrimer. However, two main situations occur depending on the energy landscape drawn by the random defects. On the one hand, for many disordered configurations, these states are explicitly localized. As a consequence, when the exciton is initially located on a surface site, its state preferentially decomposes on a localized state so that, as time elapses, the exciton stays in the neighborhood of the excited site. The spectral localization of the initially highly degenerate states thus favors a dynamical localization, as in the homogeneous case. On the other hand, for specific configurations, quasiresonances occur between particular site energies. Therefore, states initially localized on different parts of the dendrimer hybridize, resulting in the formation of new eigenstates whose extended nature is more pronounced. As a consequence, when the exciton is initially located on a surface site, its state now decomposes on a more extended state so that it becomes able to explore a larger region of the dendrimer. When an average is performed over the disorder, both kinds of configurations contribute to the dynamics, resulting in a global enhancement of the delocalized nature of the exciton when compared with what happens in a homogeneous network.

When the strength of the disorder increases, a delocalization-relocalization transition takes place. This transition results from the interplay between different mechanisms and it cannot be explained in a simple manner. For instance, we have observed that when the initial state of the exciton decomposes on an explicitly localized state in the weakly disorder regime, the transition originates in disorder-induced resonances. When W increases, the energy of the localized state shifts so that resonances occur with either almost totally symmetric extended states or states localized on other regions of the dendrimer. When one approaches the resonance, the hybridization gives rise to more extended states so that the delocalized nature of the exciton is enhanced when W increases from zero. Nevertheless, when increasing W again, that is when W becomes larger than a threshold value, one deviates from the resonance so that the localized nature of the exciton recurs. But of course, this mechanism alone does provide a clear understanding of the whole transition. Nevertheless, one thing is certain: In the strong disorder limit, the well-known Anderson localization takes place because all the exciton eigenstates clearly localize.

To conclude, let us mention that the transition observed in the present study is quite similar to the so-called inverse Anderson transition observed for noninteracting particles moving in lattices whose dynamics is governed by flatbands [51–53]. In a flatband, localized states dominate the dynamics in the weakly disordered regime so that the localization is not a consequence of the strength of the disorder but of the flatband (vanishing group velocity effect). However, when the strength of the disorder reaches a critical value, the localized states melt into extended states, resulting in a localization-delocalization transition. Note that in our case, this transition arises suddenly once the disorder turns on, that is, for a vanishing critical value of the strength of the disorder. Then, for stronger values of the disorder, an Anderson delocalization-relocalization transition appears, as observed in the present study.

V. CONCLUSION

Based on the well-known Anderson model, the dynamics of an exciton in a disordered extended dendrimer was studied numerically. The properties of the exciton were described using a standard tight-binding model in which the site energies are random variables. The corresponding time-dependent Schrödinger equation was solved numerically assuming that the exciton is initially located on a surface site of the dendrimer.

In a homogeneous network, it was shown that the dynamics is controlled by three highly degenerate energy levels. Because of the degeneracy, specific quantum interferences arise between the different paths followed by the exciton to tunnel. These interferences favor a dynamical localization so that the exciton remains confined over the few sites that surround the excited site. When the dendrimer is perturbed by random defects, we observed two regimes, depending on the strength of the disorder. In the weakly disordered regime, symmetry breaking raises the degeneracy of the relevant states. The disorder enhances the propagation of the exciton, which becomes able to explore a larger region around the excited site. These results corroborate the recent idea that, in some cases, weak disorder improves the quantum communication and facilitates the spreading of a quantum walk. Unfortunately, such an effect does not survive in the strongly disordered regime. In that case, the spectral localization of the eigenstates favors the recurrence of the dynamical localization, as expected from Anderson theory.

[1] F. Vogtle, G. Richardt, and N. Werner, *Dendrimer Chemistry: Concepts, Syntheses, Properties, Applications* (Wiley, Weinheim, 2009).
[2] J. M. J. Frechet, Science **263**, 1710 (1994).
[3] A. W. Bosman, H. M. Janssen, and E. W. Meijer, Chem. Rev. **99**, 1665 (1999).
[4] D. Astruc, E. Boisselier, and C. Ornelas, Chem. Rev. **110**, 1857 (2010).
[5] K. Harigaya, Chem. Phys. Lett. **300**, 33 (1999).
[6] K. Harigaya, Phys. Chem. Chem. Phys. **1**, 1687 (1999).
[7] K. Harigaya, Int. J. Mod. Phys. B **13**, 2531 (1999).
[8] M. A. Martin-Delgado, J. Rodriguez-Laguna, and G. Sierra, Phys. Rev. B **65**, 155116 (2002).
[9] C. Supritz, A. Engelmann, and P. Reineker, J. Lumin. **111**, 367 (2005).
[10] C. Supritz, A. Engelmann, and P. Reineker, J. Lumin. **119–120**, 337 (2006).
[11] C. Supritz, A. Engelmann, and P. Reineker, J. Lumin. **122–123**, 759 (2007).
[12] C. Supritz, V. Gounaris, and P. Reineker, J. Lumin. **128**, 877 (2008).

[13] S. Tretiak, V. Chernyak, and S. Mukamel, J. Phys. Chem. B **102**, 3310 (1998).
[14] E. Y. Poliakov, V. Chernyak, S. Tretiak, and S. Mukamel, J. Chem. Phys. **110**, 8161 (1999).
[15] V. Chernyak, E. Y. Poliakov, S. Tretiak, and S. Mukamel, J. Chem. Phys. **111**, 4158 (1999).
[16] T. Minami, S. Tretiak, V. Chernyak, and S. Mukamel, J. Lumin. **87–89**, 115 (2000).
[17] J. C. Kirwood, C. Scheurer, V. Chernyak, and S. Mukamel, J. Chem. Phys. **114**, 2419 (2001).
[18] M. Nakano, M. Takahata, H. Fujita, S. Kiribayashi, and K. Yamaguchi, Chem. Phys. Lett. **323**, 249 (2000).
[19] M. Nakano, M. Takahata, H. Fujita, S. Kiribayashi, and K. Yamaguchi, J. Phys. Chem. A **105**, 5473 (2001).
[20] M. Takahata, M. Nakano, H. Fujita, and K. Yamaguchi, Chem. Phys. Lett. **363**, 422 (2002).
[21] M. Nakano, M. Takahata, S. Yamada, K. Yamaguchi, R. Kishi, and T. Nitta, J. Chem. Phys. **120**, 2359 (2004).
[22] M. Nakano, R. Kishi, T. Minami, and K. Yoneeda, Molecules **14**, 3700 (2009).
[23] G. W. Crabtree and N. S. Lewis, Phys. Today **60**, 37 (2007).
[24] A. Bar-Haim, J. Klafter, and R. Kopelman, J. Am. Chem. Soc. **119**, 6197 (1997).
[25] M. S. Choi, T. Aida, T. Yamazaki, and I. Yamazaki, Chem. Eur. J. **8**, 2667 (2002).
[26] O. Mulken and A. Blumen, Phys. Rep. **502**, 37 (2011).
[27] A. M. Childs, Phys. Rev. Lett. **102**, 180501 (2009).
[28] A. M. Childs and J. Goldstone, Phys. Rev. A **70**, 022314 (2004).
[29] E. Agliari, A. Blumen, and O. Mulken, Phys. Rev. A **82**, 012305 (2010).
[30] E. Farhi, J. Goldstone, and S. Gutmann, Theory Comput. **4**, 169 (2008).
[31] A. M. Childs, E. Farhi, and S. Gutmann, Quantum Inf. Proc. **1**, 35 (2002).
[32] V. Pouthier, J. Chem. Phys. **139**, 234111 (2013).
[33] O. Mulken, V. Bierbaum, and A. Blumen, J. Chem. Phys. **124**, 124905 (2006).
[34] O. Mulken and A. Blumen, Phys. Rev. E **73**, 066117 (2006).
[35] X. P. Xu, J. Phys. A: Math. Theor. **42**, 115205 (2009).
[36] X. P. Xu, W. Li, and F. Liu, Phys. Rev. E **78**, 052103 (2008).
[37] P. W. Anderson, Phys. Rev. **109**, 1492 (1958).
[38] B. Kramer and A. MacKinnon, Rep. Prog. Phys. **56**, 1469 (1993).
[39] Y. Yin, D. E. Katsanos, and S. N. Evangelou, Phys. Rev. A **77**, 022302 (2008).
[40] O. Mulken, V. Bierbaum, and A. Blumen, Phys. Rev. E **75**, 031121 (2007).
[41] P. Rebentrost, M. Mohseni, I. Kassal, S. Lloyd, and A. Aspuru-Guzik, New. J. Phys. **11**, 033003 (2009).
[42] J. P. Keating, N. Linden, J. C. F. Matthews, and A. Winter, Phys. Rev. A **76**, 012315 (2007).
[43] S. R. Jackson, T. J. Khoo, and F. W. Strauch, Phys. Rev. A **86**, 022335 (2012).
[44] M. Aizenman and S. Warzel, J. Eur. Math. Soc. **15**, 1167 (2013).
[45] M. Aizenman and S. Warzel, Phys. Rev. Lett. **106**, 136804 (2011).
[46] D. J. Watts and S. H. Strogatz, Nature (London) **393**, 440 (1998).
[47] B. J. Kim, H. Hong, and M. Y. Choi, Phys. Rev. B **68**, 014304 (2003).
[48] A. Anishchenko, A. Blumen, and O. Mulken, Quantum Inf. Process **11**, 1273 (2012).
[49] D. Aharonov, A. Ambainis, J. Kempe, and U. Vazirani, in *Proceedings of the Thirty-third Annual ACM Symposium on Theory of Computing (STOC01)* (ACM Press, New York, 2001), p. 50.
[50] F. Dominguez-Adame, A. Sanchez, and E. Diez, J. Appl. Phys. **81**, 777 (1997).
[51] M. Goda, S. Nishino, and H. Matsuda, Phys. Rev. Lett. **96**, 126401 (2006).
[52] A. M. C. Souza and H. J. Herrmann, Phys. Rev. B **79**, 153104 (2009).
[53] J. T. Chalker, T. S. Pickles, and P. Shukla, Phys. Rev. B **82**, 104209 (2010).